# Achiral Calcium-Oxalate Crystals with Chiral Morphology from the Leaves of Some Solanacea Plants

by **Avital Levy-Lior**, **Steve Weiner**, and **Lia Addadi***

Department of Structural Biology, Weizmann Institute of Science, Rehovot, Israel (e-mail: lia.addadi.@weizmann.ac.il)

Dedicated to Professor *Duilio Arigoni* on the occasion of his 75th birthday

The leaves of some plants, particularly among the Solanacea, contain crystals of calcium oxalate with a peculiar chiral pseudo-tetrahedral morphology, even though the calcium oxalate crystal structure is centrosymmetric, hence achiral. We studied the morphology of these crystals extracted from the leaves of three Solanacea plants: the potato, the hot pepper, and a species of wild *Solanum*. The crystal morphology was the same in all three species. Based on the examination of more than 100 crystals from each plant, we showed that the crystal morphology is chiral with invariant chirality. We suggest that morphological chirality is induced by macromolecules during nucleation from a specific, genetically encoded crystal plane, and is further established during subsequent controlled crystal growth. This is one of few examples where it is possible to deduce a molecular mechanism for biologically induced breaking of morphological symmetry in organisms. A very high level of recognition is required by the macromolecules to allow them to distinguish between symmetry-related crystal planes. It is also surprising that this finely controlled mechanism of crystal formation, including the chiral morphology, has been conserved during evolution.

**Introduction.** – Morphological mirror symmetry is commonly observed in nature. When the morphological symmetry is broken, however, the resulting object may exist in two mirror-related, or enantiomorphous, forms. In the latter case, it is often only one particular mirror image that is induced in biology, and not the other. The term *breaking of morphological symmetry* refers here to permanently and invariantly removing from the morphology of a symmetrical object symmetry elements of the second kind such as mirror planes or centers of inversion [1]. The resulting object has a chiral morphology in the classical sense, *i.e.*, it is not super-imposable on its mirror image [2][3].

Snails are a common and classical example of morphological chirality, having spiral shells that revolve in a clockwise direction for more than 98% of the individuals of a given species [4]. Chirality is, thus, characteristic not only of the particular individual, but of the entire population. Because only one of the mirror-related morphologies exists, we refer to it as *invariant chirality*. It transpires that the direction of revolution of snail shells is determined genetically, and manifests itself as soon as at the stage of the second cellular division [5]. How this is determined is, however, not yet understood.

Other well-known examples of spiral morphology are found in the direction of juxtaposition of the leaves of some plants, or the direction of twining of various climbing plants. Notably, approximately 30% of these twine constantly in one direction [4]. This phenomenon, noted and discussed by *Darwin* [6], may have originated from environmental stimuli, such as the direction of the sunlight, but was later transformed into a genetically encoded characteristic.

Induced breaking of morphological symmetry in organisms is a dilemma that has boggled and will probably continue to boggle the minds of scholars interested in development. There are not many examples where the induced breaking of symmetry in the morphology of a biogenic object can be directly analyzed and related to an intrinsic property of the object itself. One such example is the so-called 'crystal sand' formed in the leaves of some plants. These are small crystals composed of calcium oxalate monohydrate [7].

In 1891, *Arcangeli* [8] reported his observations on *'cryptocrystalline calcium oxalate'* particles in the cells of various plants. These are most frequently found in the Solanacea family. He discussed his observations on the distribution of the particles in the plant, their size and shape, relative to the observations made by the French scientist *Vesque* (1874) and the German scientist *Kohl* (1889) a few years earlier. The particles are claimed to be whole crystals rather than crystal fragments, and the crystal morphology is described as tetrahedral, and often '*geminated*', in other words *twinned*. In 1958, *Philipsborn* and *Hodenberg* [9] re-examined the crystal sand produced in the plant *Atropa belladonna.* They found that the crystals are pseudo-tetrahedral. They noticed that mirror symmetry is absent in the crystal morphology, thus allowing for the possibility of enantiomorphous crystals. The conceptual paradox lies in the fact that the crystal structure of the calcium oxalate monohydrate (COM) crystals (monoclinic, $P2_1/n$) [10] contains elements of symmetry of the second kind, such as mirror planes, glide planes, or centers of inversion that interconvert between enantiomers and are, thus, incompatible with chiral objects [11]. In agreement with the symmetry of the crystal structure, the morphology of COM crystals produced *in vitro* is centrosymmetric. In contrast, the pseudo-tetrahedral morphology observed in crystal sand is not [9]. *Cody* and *Horner* [12] explained this paradox with twinning. Twinning, they suggested, is the reason for the crystals assuming a tetrahedral shape that should not occur in crystals with monoclinic structures. These authors did not, however, address the problem of the chiral morphology of the crystals. Indeed many, but not all of the crystals of crystal sand are twinned, as are in general COM crystals.

We recently analyzed the morphology of pseudo-tetrahedral crystals extracted from tomato and tobacco leaves, and found them to be chiral and invariant within each species [13]. We also proposed a mechanism rationalizing how the morphological reduction in symmetry can be understood within the framework of the crystal-formation process inside the cells, namely during crystal nucleation.

Here, we enlarge the scope of this research to three additional plant species; the hot pepper, the potato, and one species of wild *Solanum*. We discuss further the proposed mechanism for reduction in symmetry, together with some information that may be deduced concerning the formation of the crystals and their morphological evolution.

**Results.** – The leaves of three members of the Solanacea family of plants, known to contain crystal sand [8], *Solanum tuberosum L.* (potato plant), *Capsicum annum L.* (hot pepper), and the wild *Solanum villosum* M., were collected. Crystals were isolated by pulverization of the leaves, followed by repeated centrifugation, until a clean white pellet of crystals was obtained. The mineral type was verified as COM by IR spectroscopy.

Isolated crystals were examined in the scanning electron microscope (SEM), and the characteristic morphologies of the different crystals were noted. The population of crystals originating from each plant varied slightly, both with respect to morphology and size. In all three cases, a large proportion of the crystals were in the form of crystal sand, both as single and twinned crystals. The single crystals make up anywhere between 15 and 30% of the crystal sand population, depending on the specific plant type. Crystal twinning is easily identified either by the existence of an obvious gemination in the crystal morphology or by the presence of concave angles in the middle of crystal edges. Crystals collected from potato leaves also included a few druses (aggregates of crystals) [7], styloids (elongated needles), and prismatic-shaped crystals. The sizes of the single crystals ranged from *ca.* 1- to 5-μm. Crystals from the leaves of the pepper plant comprised many druses and a larger proportion of twinned crystals in relation to single crystals. A few calcium oxalate dihydrate crystals, recognizable by their typical octahedral morphology, were also observed. The size distribution of the single crystals was in the same range as for the crystals from the potato plant, although a few large single crystals up to *ca.* 9 μm were observed. The size distribution of single crystals extracted from the wild *Solanum* ranged from 0.8- to 3-μm, which is smaller than in the case of the other two species.

The morphologies of the single crystals from the three plants were first examined by SEM, choosing only crystals that lie on their $(10\bar{1})$ basal plane (*Fig. 1*). Approximately ten crystals from each plant were inspected (*Table*). The crystal habit was identified by first measuring the set of dihedral angles between adjoined crystal faces. The morphology was then unequivocally reconstructed by fitting the set of measurements to the known structure. Thereby, dihedral angles were measured by adjusting the orientation of the crystal such that adjoined crystal faces were observed in an 'edge-on' position (for a detailed description of these measurements, see the *Exper. Part*). Nine dihedral angles were measured per crystal, corresponding to the three angles between the lateral planes and six angles between lateral and basal planes (each measured from two directions; *Fig. 2*). The *Table* lists the final dihedral angles. The dihedral-angle measurements of crystals extracted from the potato, pepper, and the wild *Solanum* plants were very similar in that their maximum standard deviation was $\pm 2.5^\circ$, which lies well within the standard deviation of individual sets of measurements. This shows that the COM single crystals extracted from all three species had the same morphology.

The model of the morphology of the pseudo-tetrahedral crystals was constructed by combining the above data with the knowledge that the crystal rests on the $(10\bar{1})$ face, as established by *Bouropoulos et al.* through electron diffraction [13]. Note that indexing of the diffraction pattern on which our model is based, as well as all further calculations leading to the final model construction, were performed with the COM structure proposed by *Deganello* and *Piro* ($P2_1/n$; $a = 9.9763$, $b = 14.5884$, $c = 6.2913$ Å; $\beta = 107.05^\circ$) [10]. The crystal model was constructed *via* a process of trial and error with the aid of a computer program that simulates crystal morphology, based on the crystal structure and a list of *Miller* indices of the faces [14]. The crystal model established was identical to the one proposed for the COM crystals from tomato leaves, as discussed in detail in [13]. The crystal planes identified were, in addition to the basal plane $(10\bar{1})$, (101) and $(\bar{1}10)$. The third lateral plane was labeled $(\bar{h}\bar{k}0)$ because no specific crystal plane within this family had angles fitting all the measured sets. The planes closest to

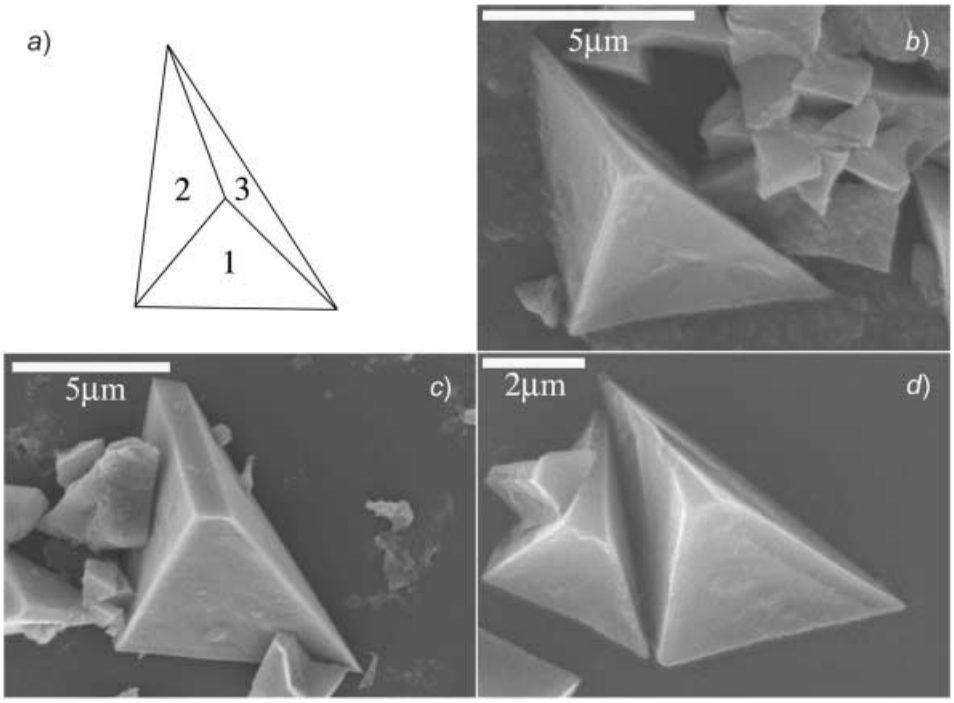


Fig. 1. *Morphological representation and electron micrographs of representative COM single crystals extracted from plant leaves.* a) *Model of the morphology of the single crystals.* Faces 1, 2 and 3 correspond to the $(h\bar{k}0)$, $(\bar{1}10)$, and (101) planes, resp. b) *Micrograph of a characteristic crystal extracted from potato leaves.* c) *Micrograph of a characteristic crystal extracted from hot pepper leaves.* The small face in the upper part corresponds to the $(\bar{1}32)$ plane. d) *Micrograph of a characteristic crystal extracted from wild* Solanum. The small face in the upper part of the crystal corresponds to the $(\bar{1}01)$ plane.

Table. *Observed* vs. *Calculated Dihedral Angles* [°] *between the Crystallographic Planes Corresponding to the Faces of Crystals Extracted from Different Plants.* The number ($n$) of crystals investigated is stated. Calculated angles correspond to the dihedral angles of the established crystal model. All measured angles have been corrected for tilt compensation (see *Exper. Part*).

| Planes ($n=12$) | Potato ($n=5$) | Pepper ($n=7$) | *Solanum* | Tomato[a]) | Calculated |
|---|---|---|---|---|---|
| $(10\bar{1})$ (101) | $69.9 \pm 3.9$ | $73.4 \pm 4.6$ | $68.3 \pm 1.0$ | $72.9 \pm 1.1$ | 63.6 |
| $(10\bar{1})$ $(h\bar{k}0)$ | $48.6 \pm 2.9$ | $49.4 \pm 1.7$ | $49.5 \pm 3.9$ | $47.0 \pm 5.4$ | – |
| $(10\bar{1})$ $(\bar{1}10)$ | $65.7 \pm 2.8$ | $64.2 \pm 1.7$ | $64.2 \pm 4.3$ | $69.3 \pm 4.2$ | 73.8 |
| $(\bar{1}10)$ $(h\bar{k}0)$ | $96.7 \pm 5.2$ | $95.5 \pm 4.0$ | $94.4 \pm 5.7$ | $96.6 \pm 2.1$ | 96.1[b]) |
| $(\bar{1}10)$ (101) | $47.7 \pm 2.8$ | $47.7 \pm 2.9$ | $46.9 \pm 3.4$ | $48.2 \pm 1.2$ | 54.4 |
| (101) $(h\bar{k}0)$ | $69.5 \pm 2.7$ | $67.5 \pm 2.2$ | $69.6 \pm 3.1$ | $69.9 \pm 4.5$ | 71.6[b]) |

[a]) Values taken from [13]. [b]) Calculated for the $(\bar{1}\bar{3}0)$ plane.

the measured set were $(\bar{1}\bar{2}0)$ or $(\bar{1}\bar{3}0)$. The calculated angles (*Table*) of the morphological model proposed differed from the angles measured up to a maximum of 10°.

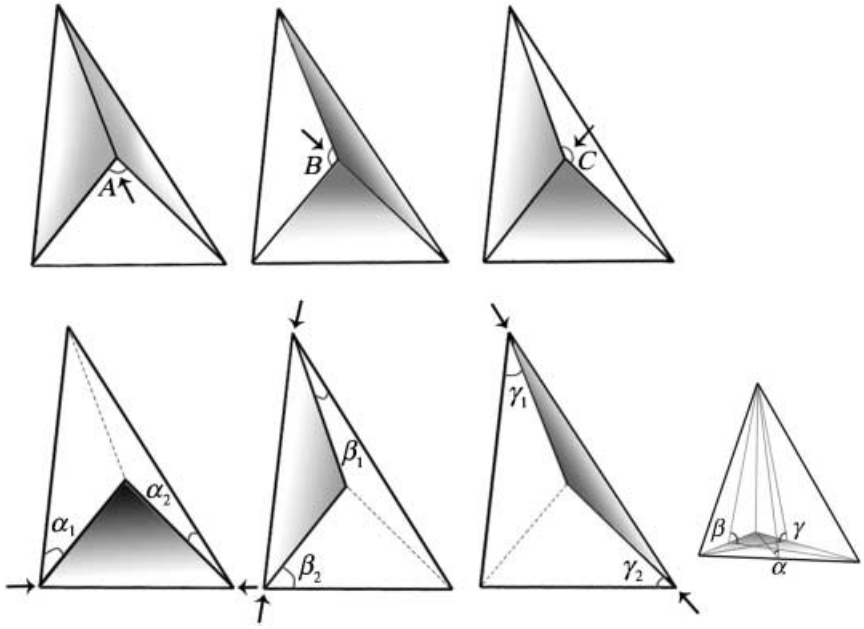


Fig. 2. *Schematic representation of the nine dihedral angles measured per crystal.* Angles *A*, *B* and *C* were determined directly from the SEM micrographs (arrows mark the intersection line between the adjoining planes defining the dihedral angle). Angles $\alpha_1$ and $\alpha_2$ were averaged to yield the dihedral angle $\alpha$. The same averaging process was performed to obtain angles $\beta$ and $\gamma$.

The morphology of the single crystals from the different plants was chiral and invariant, insofar as only one out of the two possible symmetry-related (enantiotopic) {101}[1]) and {10$\bar{1}$} faces were developed, and it was always the same face; namely the (10$\bar{1}$) and (101) faces, and not the ($\bar{1}$01) and ($\bar{1}$0$\bar{1}$) ones. Analogously, only two out of the four possible symmetry-related faces of type {*hk*0}, namely ($\bar{1}$10) and ($h\bar{k}$0), were developed. It is also essential to note that the face labeled ($h\bar{k}$0) is not of the same family as the ($\bar{1}$10) face. If this face were ($\bar{1}\bar{1}$0), the crystal morphology would not be chiral. The chirality is highlighted by the fact that it was impossible to fit the morphological model to the measured set of dihedral angles without first removing the symmetry of the monoclinic structure from the set of *Miller* indices. Note that in all three cases, moving in a clockwise direction around the crystal and beginning at the ($h\bar{k}$0) face (face 1 in *Fig. 1,a*), first the ($\bar{1}$10) face (face 2) and then the (101) face (face 3), were encountered.

Of the four faces developed in the biogenic crystals, three were expressed in the nonbiogenic COM crystal. The only face not expressed was the (101) face, which is, therefore, believed to be the key to the chiral morphology found in the biogenic crystals. *Fig. 3* Shows the morphology of a hypothetical nonbiogenic COM crystal, delimited by faces {10$\bar{1}$}, {010}, {110}, and {120}. Both the {110} and {120} faces are

[1]) Braces { } correspond to the family of symmetry-related planes, while parentheses ( ) indicate one specific plane.

commonly observed in nonbiogenic crystals [13][15]. In reality, however, nonbiogenic crystals develop either a full set of four symmetry-related {110} faces, or a full set of four symmetry-related {120} faces. We used two faces from one set, and two faces from the other to suitably derive the morphology observed in the biogenic crystals. The orientation of the (101) plane is marked within this morphology, illustrating how the development of a {101} oblique face causes a reduction in the symmetry of the COM crystals. Crystal growth from both sides of the (101) plane would create both enantiomorphs; in nature, this was not found to be the case.

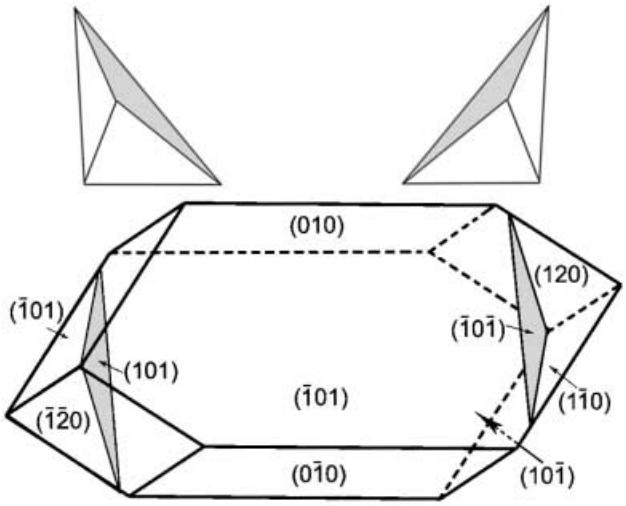


Fig. 3. *Representation of a biogenic COM single crystal* (top left) *and its theoretical enantiomorph* (top right) *superimposed on an COM single crystal* grown *in vitro* (bottom). The *in vitro* crystal morphology is centrosymmetric, with two {$\bar{1}$01} faces, two {010} faces, and four {110} or {120} faces. The crystal planes expressed in the biogenic crystal (upper left) are (10$\bar{1}$), ($\bar{1}$10), ($\bar{1}\bar{2}$0), and (101), the last-mentioned being shaded. The theoretical enantiomorph (right) has not been found in nature. It would exist if crystal growth were to occur in both directions of the shaded (101) plane, and the faces expressed would then be ($\bar{1}$01), (1$\bar{1}$0), (120), and ($\bar{1}$0$\bar{1}$).

To verify that the chiral morphology of these crystals is invariant, more than 100 single crystals were examined from each plant. All crystals were observed under identical orientations (tilt angle 0°), *i.e.*, viewed from above the crystal, looking down perpendicular to its basal plane. All were found to have the same handedness. The computer program used to construct the crystal model was applied again to see if an alternative model could be found, representing crystals with opposite morphology, but no such model, corresponding to the given constraints of the measured dihedral angles, could be found. Thus, the enantiomorph does not exist, or may be present in less than 1% of the crystals, at least in the leaves of these plants.

**Discussion.** – We have shown that three different plants belonging to the Solanacea, the potato, the hot pepper, and a local wild *Solanum* all have in their leaves crystals of calcium oxalate monohydrate (COM) with the same unusual pseudo-tetrahedral morphology. This morphology is chiral and invariant, with only one enantiomorph being formed.

The crystals found in the leaves of the tomato and tobacco plants, also members of *Solanacea*, have previously been investigated [13]. The crystals from tomato leaves share the same morphology as the one observed here. The crystals from tobacco leaves possess three faces, $(10\bar{1})$, $(\bar{1}10)$, and $(h\bar{k}0)$, identical to the previous four examples, and one differing from them. Interestingly, the latter face, (101) in the four examples above, and (102) in tobacco, is the only face that is never observed in crystals grown synthetically from solutions of calcium oxalate.

A conceivable mechanism explaining how the chiral morphology may be achieved involves nucleation of the crystals from the (101) face (or the (102) face for tobacco). The arguments supporting this proposal are that the (101) face requires specific induction in order to develop. The specific induction mechanism needs to distinguish between the (101) face and the opposite (enantiotopic) $(\bar{1}0\bar{1})$ face. If this were not the case, both enantiomorphous crystals would be observed. Such a fine level of recognition is more likely manifested during nucleation, where a small difference in the activation energy may be translated into a very large kinetic advantage [16–20]. A template can selectively nucleate a favored structure, while any other growth process would involve close competition between the rates of growth of similar faces. Furthermore, if growth of the COM crystals after nucleation occurs in the different directions with relative rates comparable to the nonbiogenic growth, the resulting morphology would be expected to match that observed in the biogenic crystals, as schematically illustrated in *Fig. 3*.

Proteins or other biological macromolecules are thought to be involved in the control of crystal nucleation in biological hard tissues [21]. Some proteins found in, *e.g.*, mollusk shells selectively nucleate aragonite or calcite crystals, depending on whether their origin is in the aragonitic or calcitic layer of the shell, respectively [22][23]. Indeed, *Bouropoulos et al.* [13] showed that the presence of proteins extracted from within the COM crystals of tomato and tobacco accelerate the formation of new COM crystals from supersaturated solutions of calcium oxalate *in vitro*. This led to the hypothesis that biological macromolecules are involved in the nucleation of COM crystals in potato, pepper, and wild *Solanum*, as well as in tomato and tobacco leaves.

Support for this hypothesis is derived from recent nucleation experiments, where crystallization was induced from supersaturated solutions in contact with hydrophobic surfaces. These hydrophobic surfaces contained adsorbed proteins extracted by dissolution of the COM crystals from potato leaves. Preliminary experiments showed that a significant proportion of the crystals, indeed, nucleate on these surfaces from the {101} plane. These preliminary experiments support the notion that there may be specific proteins adsorbed on the crystal-chamber membranes, which nucleate the crystals selectively from the (101) face. The additional level of recognition introduced by the controlled development of the $(\bar{1}10)$ and $(h\bar{k}0)$ faces would necessarily have to be introduced during the subsequent growth.

The structure of COM is shown in *Fig. 4*, where the relative orientations of the planes, developed as stable crystal faces in the pseudo-tetrahedral crystals, are indicated. The suggested nucleation plane, (101), is highlighted by the green-lined surface at the bottom of the figure. The plane is characterized by emerging $COO^-$ groups and $Ca^{2+}$ ions, which may be conceivably matched by functional groups on the templating protein. A slightly asymmetric orientation of the $COO^-$ groups relative to

the surface can be appreciated. This slight asymmetry is sufficient, in principle, to break the symmetry of the surface relative to the higher symmetry of the bulk structure. The point symmetry of the bulk crystal structure contains at least one symmetry operation of the second kind, namely mirror symmetry. The (101) surface is, however, oblique to the plane containing the mirror-point symmetry. Thus, no mirror-point-symmetry relation exists between the oxalate molecules emerging at the surface. This fundamental concept has been analyzed and demonstrated in a series of studies on synthetic crystals and crystallizations in the 1980s and early 1990s [24–28] and also more recently [29][30]. The recognition required by the macromolecules to allow them to distinguish the (101) plane from its opposite ($\bar{1}0\bar{1}$) plane, is, however, incredibly sophisticated. How this is implemented in practice is difficult to understand.

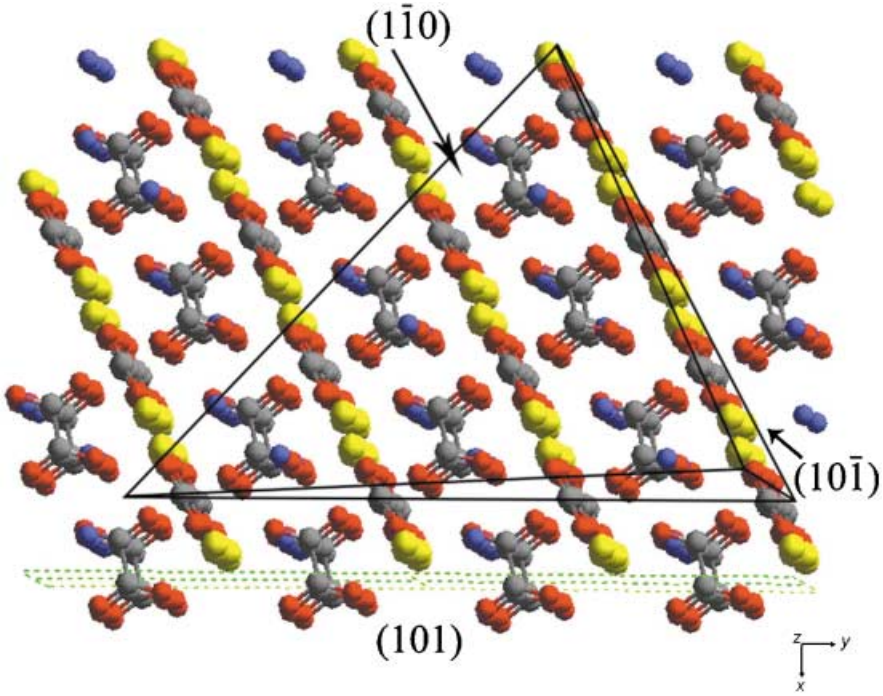


Fig. 4. *Superimposition of the COM crystal morphology on the crystalline structure.* The crystal is lying on the proposed (101) nucleation plane (indicated in green). Color code: Ca-ions, yellow; O-atoms, red; $H_2O$ molecules, blue; C-atoms, grey.

A similar mechanism of selective nucleation from a chiral crystal plane may conceivably be responsible for other examples of chiral morphologies adopted in single-crystal skeletal materials by various organisms such as certain marine sponges [31], coccoliths [32][33], and magnetotactic bacteria [34][35].

It is difficult to believe that the specific enantiomorph developed in all these cases represents some intrinsic advantage for the organism over the opposite enantiomorph. The fact that only one enantiomorph is developed indicates, however, that the chiral morphology is probably genetically encoded. Evidence that calcium oxalate crystal

morphology is genetically encoded in plants was recently obtained, showing that mutations in plant genes cause crystals with modified morphologies to be produced [36]. Even accepting this, it is noteworthy that the same morphology with the same invariant chirality is conserved over the four plant species that were studied here. In particular, note that potato, tomato, and pepper plants have been domesticated, whereas *Solanum villosum* is a wild plant.

These findings appear to indicate that the crystals must have a specific function, if the mechanism of formation of the crystals, including the chiral morphology, is so conserved. The function of the COM crystals in plants is still a subject of debate. They are believed by some investigators to provide a means for the plant to get rid of an unwanted metabolic side product. In other words, packaging the material in crystals would provide an efficient way of 'waste disposal'. The packaging mechanism and the morphology appear to be, however, finely controlled. We can only surmise that such a sophisticated mechanism, genetically encoded and conserved in a variety of plants, is unlikely to have a nonspecific function.

## *Experimental Part*

*General*. Potato (*Solanum tuberosum L.*) leaves were collected from the greenhouse of the Department of Plant Science of the Weizmann Institute of Science. *Solanum villosum* M. leaves were collected from a local garden, and hot pepper (*Capsicum annum L.*) leaves were collected from plants purchased at a local greenhouse and grown in the laboratory. Leaves were gathered year round.

*Extraction of Calcium Oxalate Crystals.* Fresh leaves (*ca.* 300 g) were thoroughly washed with tap water and then with deionized water (DW). They were then treated with a 1 mM aq. soln. of sodium azide ($NaN_3$; *Merck*) for 2 h, washed with DW and air-dried. The dry leaves were blended in a laboratory blender (*Waring*) for 5 min, while continuously adding anh. EtOH (*Bio-Lab*) to a total volume of 300 ml to prevent dissolution of the crystals. The resulting mixture was filtered through cloth gauze to remove coarse org. material. The org. suspension was placed in 50-ml centrifuge tubes and centrifuged at 4000 rpm for 5 min at 4° (*Eppendorf 5810R*). The supernatant was removed, the pellet was resuspended (*Vortex-genie 2*) in anh. EtOH and centrifuged again (as above). This was repeated two to four times with anh. EtOH, until a clean pellet was obtained. The same procedure was performed three more times with DW and, finally, three more times with an aq. soln. (1.7 g $ml^{-1}$) of sodium polytungstate ($Na_6(H_2W_{12}O_{40})\cdot H_2O$; *Sometu-Europe*). The pellet was then washed twice with DW, once with anh. EtOH, and allowed to dry in air. The purity of the crystals was determined by FT-IR spectroscopy on a *Prospect* apparatus (*Midac*). The absorptions corresponding to COM are at 1620, 1318, 949, 884, 782, 666, and 516 $cm^{-1}$. In calcium oxalate dihydrate, the peaks at 1620 and 1318 $cm^{-1}$ are shifted to 1643 and 1324 $cm^{-1}$, resp.

*Scanning Electron Microscopy* (SEM). Specimens were prepared by placing a drop of dilute crystal suspension on glass slides and allowing the crystals to dry in air. Glass slides were attached to aluminum SEM stubs by carbon-coated double-adhesive tape, sputter coated with gold, and examined in a *Jeol JSM-6400* scanning electron microscope.

*Dihedral-Angle Measurements.* Dihedral angles were measured from SEM images. To measure each angle, the adjoined planes creating it must be brought to an 'edge-on' position, which is reached through a combination of rotations and translations of the specimen in the *xy* plane, as well as by tilting the microscope stage relative to this plane, until both crystal faces delimiting the dihedral angle of interest just disappear from view. The apical angles *A*, *B*, and *C* (see *Fig. 2*) were measured directly from the SEM micrographs by the following procedure. Angles $\alpha$, $\beta$, and $\gamma$ were calculated by averaging between pairs of measurements of each dihedral angle, performed from its two sides:

$$\alpha = \frac{\alpha_1 + \alpha_2}{2}, \beta = \frac{\beta_1 + \beta_2}{2}, \gamma = \frac{\gamma_1 + \gamma_2}{2}$$

The maximum tilt angle allowed in the microscope was restricted to 75°, where, in fact, a 90° tilt is necessary for an accurate measurement of the angles between lateral and basal faces. A correction of these angles was, thus, essential to compensate for the systematic tilt-angle limitation of the electron microscope. The systematic

correction needed was worked out geometrically to be $\tan^2\alpha_{calc.} = \tan^2\alpha_{obs.}/\cos^2\xi$, where the angle $\xi$ corresponds to the additional angle needed to reach a tilt of $90°$, in this case $15°$; this corresponds to $\alpha_{calc.} = 1.035\ \alpha_{obs.}$. The correction was of the order of $2.5°$ and did not change the identified crystallographic planes.

*Crystal-Model Construction*. The crystal model was constructed through a process of trial and error, with the aid of the computer program SHAPE [14]. Tentative assignments were made by finding which faces form with the $(10\bar{1})$ basal plane dihedral angles within the measured values. The angles *A*, *B*, and *C* (see *Fig. 2*) were then checked. The process was repeated iteratively, until a model was found that matched all the values measured. The final model represents the closest combination of crystal faces corresponding to the angles from the exper. data set. All other crystal-face combinations deviated substantially from the combination of angles arrived at experimentally. In particular, no combination of faces could be found to match the observed data set, when starting from a basal plane $(\bar{1}01)$ rather than $(10\bar{1})$.

We thank *Elisha Tel-Or*, *Yair Ream*, *Zohar Hajbi*, and *Chalfon Bookra* for their help in finding, identifying, and growing the plants. *S. W.* is the incumbent of the Dr.-Trude Burchardt-professorial chair of Structural Biology, and L.A. is the incumbent of the Dorothy-and-Patrick-Gorman professorial chair of Biological Ultrastructure. This work was supported by a grant from the *Israel Science Foundation* under the auspices of the *Israel Academy of Sciences and Humanities*.

## REFERENCES

[1] K. Mislow, P. Bickart, *Isr. J. Chem.* **1977**, *15*, 1.
[2] L. Pasteur, *Ann. Chem. Phys.* **1848**, *24*, 442.
[3] W. T. Kelvin, 'Baltimore lectures on molecular dynamics and wave theory of light', C. J. Clay & Sons, London, 1904.
[4] T. A. Cook, 'The curves of life', Constable and Company, London, 1914.
[5] G. Freeman, J. W. Lundelius, *Wilhelm Roux's Arch.* **1982**, *191*, 69.
[6] C. Darwin, 'The origin of species', John Murray, 1859.
[7] V. R. Franceschi, H. T. Horner, *Bot. Rev.* **1980**, *46*, 361.
[8] G. Arcangeli, *Bull. D. Soc. Bot. Ital.* **1891**, 867.
[9] H. V. Philipsborn, R. F. V. Hodenberg, *Protoplasma* **1958**, *49*, 320.
[10] S. Deganello, O. E. Piro, *Neues Jb. Miner. Monat.* **1981**, *2*, 81.
[11] L. Addadi, M. Geva, *Cryst. Eng. Commun.* **2003**, *5*, 140.
[12] A. M. Cody, H. T. Horner, *Am. J. Bot.* **1985**, *72*, 1149.
[13] N. Bouropoulos, S. Weiner, L. Addadi, *Chem.–Eur. J.* **2001**, *7*, 1881.
[14] E. Dowty, SHAPE, Program for calculating and displaying the morphology and symmetry of crystals, Shape Software, 2001.
[15] A. Millan, *Cryst. Growth Des.* **2001**, *1*, 245.
[16] I. Weissbuch, L. Addadi, L. Leiserowitz, M. Lahav, *J. Am. Chem. Soc.* **1988**, *110*, 561.
[17] E. M. Landau, M. Levanon, L. Leiserowitz, M. Lahav, J. Sagiv, *Nature (London)* **1985**, *318*, 353.
[18] E. Landau, R. Popovitz-Biro, M. Levanon, L. Leiserowitz, M. Lahav, J. Sagiv, *Mol. Cryst. Liq. Cryst.* **1986**, *134*, 323.
[19] S. Mann, B. R. Heywood, S. Rajam, J. D. Birchall, *Nature (London)* **1988**, *334*, 692.
[20] M. Gavish, R. Popovitz-Biro, M. Lahav, L. Leiserowitz, *Science* **1990**, *250*, 973.
[21] L. Addadi, S. Weiner, *Proc. Natl. Acad. Sci. U.S.A.* **1985**, *82*, 4110.
[22] G. Falini, S. Albeck, S. Weiner, L. Addadi, *Science* **1996**, *271*, 67.
[23] A. M. Belcher, X. H. Wu, R. J. Christensen, P. K. Hansma, G. D. Stucky, D. E. Morse, *Nature (London)* **1996**, *381*, 56.
[24] L. Addadi, Z. Berkovitch-Yellin, I. Weissbuch, M. Lahav, L. Leiserowitz, S. Weinstein, *J. Am. Chem. Soc.* **1982**, *104*, 2075.
[25] I. Weissbuch, L. Addadi, Z. Berkovitch-Yellin, E. Gati, M. Lahav, L. Leiserowitz, *Nature (London)* **1984**, *310*, 161.
[26] J. M. McBride, S. B. Bertman, *Angw. Chem., Int. Ed.* **1989**, *28*, 330.
[27] I. Weissbuch, L. Addadi, M. Lahav, L. Leizerowitz, *Science* **1991**, *253*, 637.
[28] L. Addadi, Z. Berkovitch-Yellin, I. Weissbuch, M. Lahav, L. Leiserowitz, in 'Topics in Stereochemistry', Ed. E. L. Eliel, S. H. Wilen, N. L. Allinger, John Wiley & Sons, 1986.
[29] J. Paquette, R. J. Reeder, *Geochim. Cosmochim. Acta* **1995**, *59*, 735.

[30] C. A. Orme, A. Noy, A. Wierzbicki, M. T. McBride, M. T. Grantham, H. H., P. M. Dove, J. J. DeYoreo, *Nature (London)* **2001**, *411*, 775.
[31] J. Aizenberg, J. Hanson, T. Koetzle, L. Leiserowitz, S. Weiner, L. Addadi, *Chem.–Eur. J.* **1995**, *1*, 414.
[32] J. R. Young, J. M. Didymus, P. R. Bown, B. Prins, S. Mann, *Nature (London)* **1992**, *356*, 516.
[33] J. M. Didymus, J. R. Young, S. Mann, *Proc. R. Soc. Lond. B* **1994**, *258*, 237.
[34] S. Mann, N. H. C. Sparks, R. P. Blakemore, *Proc. R. Soc. Lond. B* **1987**, *231*, 477.
[35] S. Mann, R. B. Frankel, in 'Biomineralization: Chemical and Biochemical Perspectives', Ed. S. Mann, J. Web, R. J. P. Williams, VCH, Weinheim, 1989.
[36] M. M. McConn, P. A. Nakata, *Planta* **2002**, *215*, 380.

*Received September 29, 2003*